Hindawi
Journal of Nanomaterials
Volume 2022, Article ID 2512223, 10 pages
https://doi.org/10.1155/2022/2512223

Research Article

Ultrasonic Synthesis of Al-SBA-15 Nanoporous Catalyst for *t*-Butylation of Ethylbenzene

Azhagapillai Prabhu,[1] **Venugopal Sudha**,[2] **Muthusamy Poomalai Pachamuthu**,[3] **Balachandran Sundaravel**,[4] **and Stefano Bellucci**[5]

[1]*Department of Chemistry, Khalifa University, P.O. Box 127788, Abu Dhabi, UAE*
[2]*Department of Chemistry, Anna University, Chennai 600 025, India*
[3]*Department of Chemistry, Integrated AI & Sensors Lab, Bannari Amman Institute of Technology, Tamil Nadu-638401, Sathyamangalam, India*
[4]*School of Advanced Sciences-Department of Chemistry, Kalasalingam Academy of Research and Education, Tamil Nadu-626 126, Krishnankoil, India*
[5]*INFN-Laboratori Nazionali di Frascati, Via E. Fermi 54, 00044 Frascati, Italy*

Correspondence should be addressed to Azhagapillai Prabhu; azhagapillai.prabhu@ku.ac.ae

Received 19 November 2021; Revised 28 January 2022; Accepted 3 February 2022; Published 9 March 2022

Academic Editor: Balachandran Jeyadevan

Mesoporous Al-SBA-15 (Si/Al = 25) catalysts were synthesised by the ultrasonic (US) irradiation method at different time durations (1, 3, and 5 h) using the pluronic P123 triblock copolymer as a template. The synthesised catalysts were examined in detail by XRD, ICP-AES, N_2 adsorption-desorption, SEM, TEM, FT-IR, and TGA characterization techniques. The characterization results reveal that the catalysts possess a well-ordered hexagonal mesoporous structure. The catalytic activity of synthesised materials was investigated in the *tert*-butylation of ethylbenzene at different reaction conditions, and their identified products are *para-tert*-butylethylbenzene (*p-tert*-BEB) and *meta-tert*-butylethylbenzene (*m-tert*-BEB). It was found that high ethylbenzene conversion (69%) is achieved at 200°C with high selectivity towards *p-tert*-butylethylbenzene (80%). The optimum feed ratio (ethylbenzene: t-butyl alcohol) was 1 : 2, and the feed rate was 2 ml/h for high conversion and product selectivity. All these synthesised Al-SBA-15 (US) catalysts are compared with hydrothermally synthesised Al-SBA-15 (HT) at the same reaction conditions.

1. Introduction

Heterogeneous solid acid catalysts with mesoporous structures have been employed in many industrial chemical processes as eco-friendly nanocatalysts. Given this, many studies on mesoporous solid acid catalysts have been conducted [1–4]. Remarkably, many researchers have reported on the synthesis, functionalisation, and catalytic applications of ordered mesoporous materials (OMM) such as MCM-41, MCM-48, SBA-15, SBA-16, and KIT-6 [5–8]. Among mesoporous materials, silica-based catalysts such as SBA-15 are promising in adsorption, bio-sensing, catalysis, and drug delivery applications due to their large specific surface area, narrow pore size distribution, tunable pore size, and hydrothermal stability [9, 10]. The synthesis condition and degree of silica polymerization played a considerable impact on the pore diameter and hydrothermal stability of SBA-15 [11]. Besides, the thermal ageing process of SBA-15 mainly influences the pore wall and pore sizes [12]. When compared to mesoporous MCM-41 and other silica materials, SBA-15's thicker walls greatly enhance its thermal and hydrothermal stability [13]. Though SBA-15 has excellent textural parameters, it cannot be used as such for catalytic applications due to its pure siliceous neutral network. Moreover, in situ insertion of heteroatoms into the SBA-15 framework is very difficult due to the highly acidic synthesis condition of SBA-

15. Many synthesis methods have been used to incorporate metal ions (M^{x+}) like aluminium, titanium, and vanadium into the framework [14–19]. Remarkably, the ultrasonic synthesis process is an effective method for creating mesoporous materials with unique characteristics [20–24]. Under highly acidic conditions, MCM-41 was synthesised using ultrasonic irradiation over a wide range of irradiation strengths in a short amount of time [25]. Lee et al. have reported the SBA-15 and Ti-SBA-15 synthesis using a fast-ultrasonic method [26]. Further, many metal oxides have also been prepared by utilising ultrasonic irradiation [27]. A mesoporous crystalline CdS nanoparticle was synthesised using the ultrasonication method with an excellent pore size ranging from 4–6 nm [28]. Wang et al. have reported that aluminium atoms are highly incorporated into the silica framework during AlMCM-41 preparation under ultrosonic irradiation, due to strong agitation and restriction of alumina formation [29].

Aluminium modified mesoporous materials such as MCM-41, SBA-15, KIT-6, and TUD-1 have been reported as solid acid catalysts for multicomponent reactions, biomass conversion, and Friedel-Craft alkylation/acylation type reactions [29–32]. Since the aluminium-based silicate meosporous catalyst possesses both Bronsted and Lewis acid sites, it is catalytically active in alkylation type reactions. Essentially, alkylation of alkyl aromatics is a commercially important reaction, and the alkylated products are used in the production of a variety of products. The vapour phase alkylation of ethylbenzene with tert-butyl alcohol was carried out over a Al-MCM-41 mesoporous catalyst [33]. The resulting *t*-butylated ethylbenzenes (*p*-alkylated ethylbenzene) serve as raw materials for the production of *t*-butylated vinylbenzene, which results in polymers with increased plasticity [34], and many studies have reported the Al-SBA-15 catalyst with superior performance in the acid-catalyzed alkylation reactions [35–39]. To the best of our knowledge, there are no reports on the use of the ultrasonication method to synthesise Al-SBA-15 in vapour phase ethylbenzene tertiary butylation reactions. In the present work, ultrasonic synthesis of Al-SBA-15 with a Si/Al ratio of 25 has been investigated. Also, a well-ordered mesoporous Al-SBA-15 (25) synthesis using ultrasonication and hydrothermal techniques is discussed. These materials were characterised by different characterization techniques, and their catalytic activities were examined in an ethylbenzene *tert*-butylation reaction with various reaction parameters.

2. Experimental

2.1. Materials and Chemicals. Aluminium isopropoxide, tetraethylorthosilicate (TEOS), hydrochloric acid (HCl), ethylbenzene, and tert-butyl alcohol were received from Merck (India) and used as received without additional purification. Pluronic P123 ($EO_{20}PO_{70}EO_{20}$; Aldrich, m.wt. 5800) was used as structure-directing agent. Double distilled water was used in all experiments.

2.2. Synthesis of Al-SBA-15 by Hydrothermal H2O. Al-SBA-15 was made with the following molar gel composition: TEOS: (0.095) Al (OiPr) 3: (6) HCl: (154) H2O: (0.148) P123.4 g of Pluronic P123 was mixed with 30 ml of water in a PP bottle and kept for vigorous stirring until a clear solution was obtained (~4 h). The solution was then added to 120 ml of 0.2 M hydrochloric acid and agitated for another 2 h, after which TEOS and the required amount of aluminium source were added into the same solution mixture and agitated at 40°C for 24 h. The solution mixture was slowly heated to a maximum of 100°C for the ageing process in a hot air oven for 24 h. Finally, the obtained solid was filtered and washed several times with deionized water before being dried overnight at 100°C and calcined for 6 h at 550°C under static air. A pure white solid was obtained after the calcination and is denoted as Al-SBA-15 (HT).

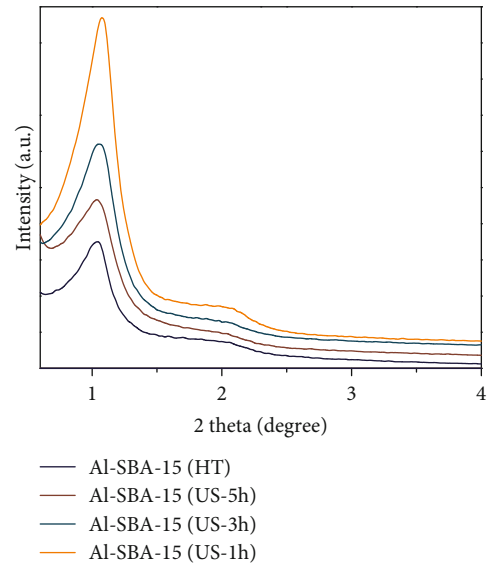

Figure 1: Low-angle XRD patterns of Al-SBA-15 (HT), Al-SBA-15(US-1 h), Al-SBA-15 (US-3 h), and Al-SBA-15 (US-5 h).

2.3. Synthesis of Al-SBA-15 by Ultrasonication (US). 4 g of pluronic P123 was mixed with 30 ml of distilled water, and after 4 h of continuous stirring, a clear solution was obtained. Then, 120 ml of 0.2 M HCl was added to it, and the solution was stirred for another 2 hrs. TEOS and the required amount of aluminium source were added, and the solution was stirred at 40°C for 24 h. The mixture was ultrasonicated for different sonication time durations (1, 3, and 5 h) using a commercial ultrasonic bath (Enertech Fast Ultrasonicator) at 30°C. Upon sonication, the solid product was recovered by filtration, washed with deionized water, and dried overnight at 100°C. Finally, the mixture was calcined at 550°C for 5 h to get the pure template-free catalyst. The synthesised Al-SBA-15 (25) is referred to as Al-SBA-15 (US-1), Al-SBA-15 (US-3), and Al-SBA-15 (US-5), where US represents ultrasonic irradiation, and 1, 3, and 5 indicate the ultrasonication time in hours.

2.4. Material Characterization. Powder XRD measurements were taken on a Bruker D8 diffractometer using Cu K ($\lambda = 1.5418Å$) radiation at a voltage of 40 kV and a current

Table 1: Structural and textural parameters of Al-SBA-15 (25).

Catalyst	d-Spacing (nm)	a_0[1] (nm)	Si/Al[2] (gel)	S_{BET}[3] ($m^2\ g^{-1}$)	Vp[4] ($cm^3\ g^{-1}$)	d_p[5] (nm)
Al-SBA-15 (US-1 h)	7.14	16.42	29	728	1.07	6.1
Al-SBA-15 (US-3 h)	7.37	17.02	28	780	1.11	6.5
Al-SBA-15 (US-5 h)	7.49	17.45	29	804	1.23	6.7
Al-SBA-15 (HT)	8.47	19.56	28	699	1.15	7.8

[1]Unit cell parameter calculated from the formula $a_0 = d_{211}$ X$\sqrt{6}$. [2]ICP-AES. [3]Specific surface area. [4]Pore volume. [5]Pore diameter.

of 40 mA. ICP-AES aluminium content was conducted using a Labtum Plasma 8440. The nitrogen adsorption and desorption experiments were carried out using a Quantachrom (QuadrasorbSI) porosimeter at 77 K, and the catalysts were degassed at 250°C for 6 h before the measurement. Thermogravimetric analysis of this as-synthesised Al-SBA-15 material was carried out using a thermogravimetric analyzer (TGA) (SDT Q600, TA Instruments, Inc.,). The sample was heated in a nitrogen flow at a temperature of 40–700°C at a heating rate of 10°C min^{-1}. A Hitachi COM- S-4200 with a 16 kV accelerating voltage was used to capture SEM micrographs. The transmission electron microscopic (TEM) images were recorded using a JEOL3010 instrument with a UHR polepiece (voltage of 300 kV). FT-IR spectra were recorded on a Bruker Tensor spectrometer using KBr pellets at a resolution of 4 cm^{-1} and 100 scans.

2.5. Vapour Phase Catalytic Reaction. At atmospheric pressure, Al-SBA-15 catalytic vapour phase alkylation of ethylbenzene with *tert*-butanol was carried out in a fixed bed vertical flow reactor (40 cm × 2 cm) [33]. The reactor kept inside the tubular furnace was heated at different temperatures using a digital temperature controller. A Pyrex glass reactor tube was packed with glass beads and quartz wool on either side of the tube to hold about 0.5 g of catalyst. A syringe pump was used to introduce the reactants into the reactor at various flow rates, and the final products were collected at the bottom of the reactor. The products were collected at a time interval of 1 h and analyzed. The liquid products were analyzed by gas chromatography (GC, Shimadzu 17) equipped with a cross-linked 5% phenylmethyl siloxane capillary column and an FID detector (N_2 as carrier gas). The products were then identified using a helium carrier gas and GC-MS (Perkin-Elmer Turbo Mass Spectrometer, EI).

3. Results and Discussion

3.1. Catalyst Characterization Results. The low angle XRD patterns of Al-SBA-15 (US 1, 3, and 5 h) and Al-SBA-15 (HT) are depicted in Figure 1. The XRD figure shows that a clear indication of all the catalysts is well-resolved diffraction peaks which are indexed to (100), (110), and (200) reflections, representing the presence of hexagonal space group P6mm. By comparing such intense patterns with those of reported patterns, the crystallisation of Al-SBA-15 via hydrothermal treatment was found to be good [30]. Similar low angle diffraction peaks were observed for metal modified SBA-15, indicating hexagonally ordered mesoporous materials [35, 36]. The d_{100} spacing and lattice parameter (a_0) values are also calculated and presented in Table 1. Furthermore, the elemental analysis (ICP-AES) showed that the Si/Al ratio obtained for Al-SBA-15 (US) and Al-SBA-15 (HT) after calcination is close to that in the synthesis gel. Remarkably, the synthesis conditions that followed led to the higher Al incorporation in the SBA-15 lattice. Furthermore, the crystallisation process was nonstoichiometric, and at mild acidic conditions, Al dissolution was limited. Since the dissolution of Al-O-Si groups is influenced by acid conditions throughout the entire reaction, the Si/Al ratio of all ultrasonication materials values was nearly identical [29].

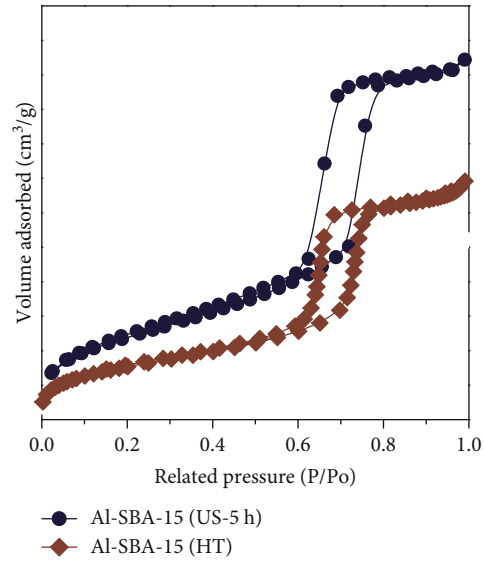

Figure 2: Nitrogen adsorption-desorption isotherm of Al-SBA-15 (US-5 h) and Al-SBA-15 (HT).

The N_2 sorption isotherms for Al-SBA-15 (US-5 h) and Al-SBA-15 (HT) are shown in Figure 2, and the textural parameters of all the synthesised Al-SBA-15 catalysts are presented in Table 1. The isotherms exhibit class IV type with a sharp capillary condensation step at high P/P0 and a H1 hysteresis loop, which are the characteristics of periodical mesopores with a honeycomb structure [35, 36]. Al-SBA-15 materials have specific surface areas of 699–804 m^2/g and pore volumes of 1.07–1.23 cm^3/g. The pore diameter ranges (6.1–7.8 nm) of the mesoporous Al-SBA-15 catalysts confirmed the mesostructure by the IUPAC porous material classification. However, ultrasonication method Al-SBA-15 samples showed a higher surface area compared with Al-SBA-15 (HT). This could be attributed to the higher amount of aluminium is incorporated into

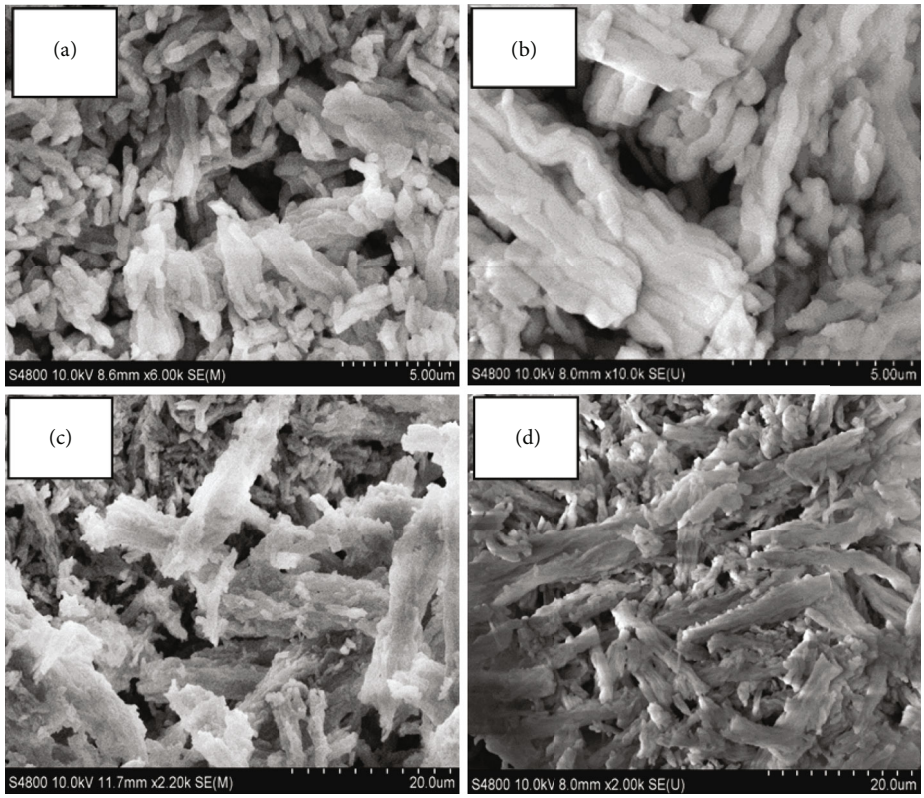

Figure 3: SEM images of Al-SBA-15: (a) HT; and US: (b) 1 h, (c) 3 h, and (d) 5 h.

the siliceous SBA-15 framework during the ultrasonication and calcination processes, which may lead to low pore wall thickness [29].

The SEM images of Al-SBA-15 (HT) and Al-SBA-15 (US-1, 3, and 5 h) are displayed in Figure 3. Al-SBA-15 (HT) is tightly packed and highly interconnected, with windows opening from each mesopore into its surrounding silica particles [30]. The SEM image of US (1 h) reveals highly irregular morphologies due to the random growth of crystals in different directions. This irregular rod-like morphology does not resemble that of Al-SBA-15 (HT). The SEM picture of Al-SBA-15 (US 3 and 5 h) also clearly shows the formation of fiber-like or rope-like morphology with 10–30 μm in length [40].

The TEM images of Al-SBA-15 (HT) and Al-SBA-15 (US-3 h) are shown in Figure 4, clearly representing the well-ordered regular arrangements of the hexagonal mesoporous structure [35]. The regularity of these mesopores is not affected after the incorporation of the Al ions into the SBA-15 materials. Besides, the TEM images clearly show that both ultrasonic and hydrothermally synthesised Al-SBA-15 materials are highly porous with a pore diameter range of 6–8 nm, and these results were in good agreement with the nitrogen sorption analysis results.

The FT-IR spectra of Al-SBA-15 (HT) and Al-SBA-15 (US-1, 3, and 5 h) in the range of 4000 cm^{-1} to 400 cm^{-1} are displayed in Figure 5. In the spectra of Al-SBA-15, the template –CH_2 vibrations are clearly seen just below 3000 cm^{-1}, and the –OH stretching of water and surface silanol (Si-O-H) group is noticed close to 3400 cm^{-1}. Further, the –OH bending vibration at about 1630 cm^{-1} is very well-confirmed [30, 40]. The intense peak close to 1200 cm^{-1} is due to framework asymmetric Si-O-Si and Si-O-Al vibrations. The corresponding symmetric vibrations occur below 1000 cm^{-1} as a weak peak. Also, the peak due to Si-O-Si bending modes was observed at 750 cm^{-1}. The spectrum due to the calcined sample shows an intense broad peak between 2800 and 3800 cm^{-1}, and it is assigned to defective Si-O-H stretching. The framework vibration due to Si-O-Si and Si-O-Al is observed at 1000, 950, and 750 cm^{-1} which are common to both hydrothermal and ultrasonic materials [39].

Figure 6 shows the TGA of as-synthesised Al-SBA-15 (US-3 h) and Al-SBA-15 (HT) samples. The trace due to the as-synthesised sample illustrates the oxidative decomposition of the losing template starting at about 175°C, and this weight loss extended up to 300°C. It is followed by an additional weight loss ascribed to the decomposition of the residual fragments. From this phase, the weight loss calculated was about 51%, which is common for all as-synthesised mesoporous structured materials. The TGA trace due to the calcined sample illustrates the weight loss below 160°C, which is attributed to adsorbed water, and it is evidence for the incorporation of aluminium into framework positions, generating Bronsted acid sites. Furthermore, the pyridine adsorbed FTIR was carried out for the catalyst and the

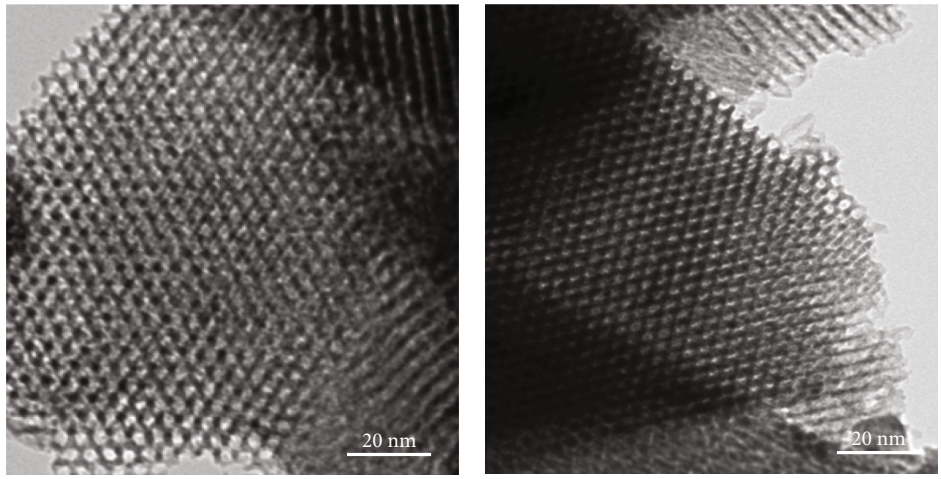

Figure 4: TEM images of (a) Al-SBA-15 (US-3 h) and (b) Al-SBA-15 (HT).

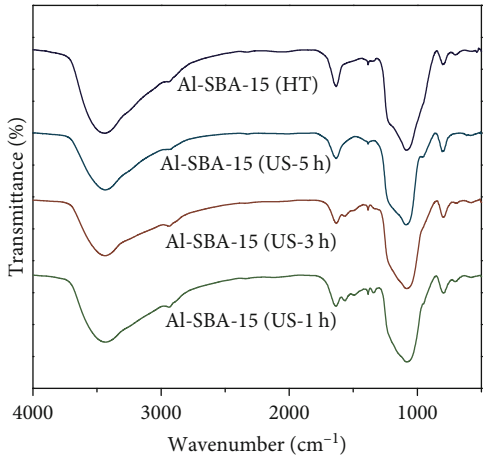

Figure 5: FTIR of Al-SBA-15 (US) and (HT) samples.

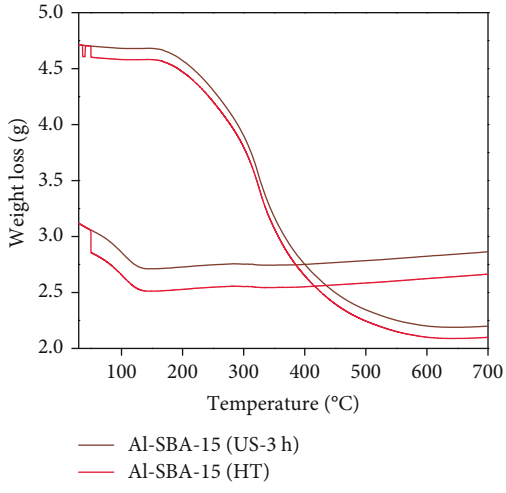

Figure 6: TGA of Al-SBA-15 (US-3 h) and Al-SBA-15 (HT).

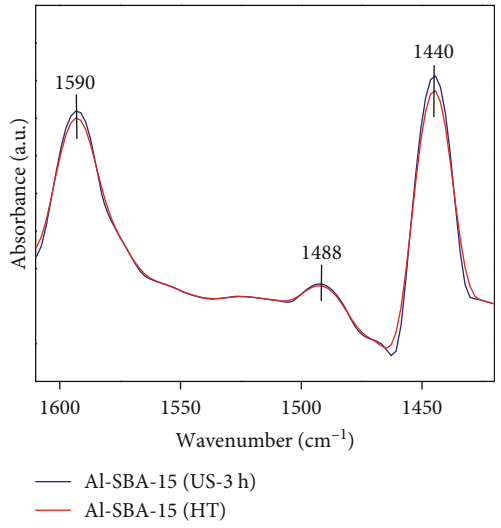

Figure 7: Pyridine-FTIR of Al-SBA-15 (US-3 h) and Al-SBA-15 (HT).

result is depicted in Figure 7. The sample showed the bands at 1590 cm^{-1}, 1488 cm^{-1}, and 1440 cm^{-1} corresponding to the Lewis and Bronsted acid sites in the Al-SBA-15 (US-3 h) sample [30].

3.2. Catalytic Performances. Over Al-SBA-15 (US) and Al-SBA-15 (HT) catalysts, vapour phase tert-bulyation of ethylbenzene with t-butanol was carried out. The obtained products were found to be p-tert-butylethylbenzene (p-tert-BEB) and m-tert-butylethylbenzene (m-tert-BEB) (Scheme 1). In addition to this, di-tert-butyl ether and other unidentified products were noticed. The reaction parameters were optimised for maximum ethylbenzene conversion and high selectivity for p-tert-BEB. The effects of feed ratio, temperature, WHSV, and different catalysts on conversion and product selectivity were examined, and the results are given below.

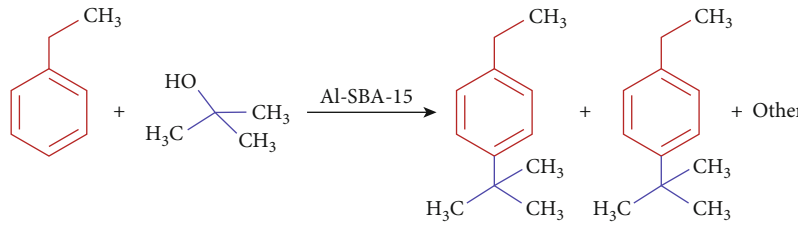

Scheme 1: Tert-butylation of ethylbenzene over Al-SBA-15 catalyst.

The effects of temperature on ethylbenzene conversion and product selectivity are depicted in Figure 8. At 175, 200, and 250°C, *tert*-Butylation of ethylbenzene over Al-SBA-15 (US-1 h) was performed with a feed ratio of 1 : 2 (ethylbenzene: *t*-butanol) and WHSV 3.30 h^{-1}.Notably, the conversion of ethylbenzene increased and then decreased with an increase in temperature from 170 to 250°C. After 175°C, the conversion was found to be less, due to the inactivated *t*-butanol yielding a *tert*-butyl cation. Furthermore, at 250°C, active site blocking by polybutene or coke reduces conversion and *p-tert*-BEB selectivity [41]. Similarly, coke formation has been reported for Al-MCM-41 and Al-SBA-15 mesoporous catalysts in vapour phase reactions [33, 36]. Here, the formation of coke was physically verified but not with any instrumental technique. Besides, isomerization at 175°C has been confirmed to a very small extent by feeding *p-tert*-BEB over the surface of the catalyst. As a result of the isomerisation of *p-tert*-BEB into thermodynamically favorable *m-tert*-BEB, the selectivity of *p-tert*-BEB decreased with increasing temperature. A similar observation was made by Sakthivel et al. for Al-MCM-41 [42]. According to the findings, the optimal temperature for ethylbenzene conversion (72%) is 200°C.

The formation of *m-tert*-BEB is proposed to proceed by isomerization of *p-tert*-BEB. The isomerization can be suppressed by increasing the flow rate as it is a time-dependent process. The effect of flow rate was studied at 200°C, and the results are shown in Figure 9. The conversion of ethylbenzene decreases with the increase in flow rate from 2 ml/h to 4 ml/h. When *t*-butanol and ethylbenzene diffuse through pores, the alcohol is absorbed first, followed by the substrate [42]. There is a release of steric strain when tetrahedral *t*-butanol is chemisorbed on the Brønsted acid sites to form a steric-free trigonal planar *tert*-butyl cation [37, 41]. So, the decrease in the conversion of ethylbenzene with an increase in flow rate is due to the rapid diffusion of *t*-butanol without much chemisorption on the Brønsted acid sites [43]. With an increase in flow rate, the selectivity of *m-tert*-BEB decreases, indicating that the product is generated solely *via* the isomerization of *p-tert*-BEB rather than by a direct electrophilic process [43]. The optimised reaction condition of 2 ml/h is the best flow rate for the conversion of ethylbenzene and selectivity of *p-tert*-BEB.

The effect of feed ratio on conversion and product selectivity was studied at 200°C with a flow rate of 2 ml/h, and the results are presented in Figure 10. The conversion of ethylbenzene increases from 1 : 1 to 1 : 2, but at 1 : 3 and 1 : 4, it is found to be decreased. The increase in conversion from

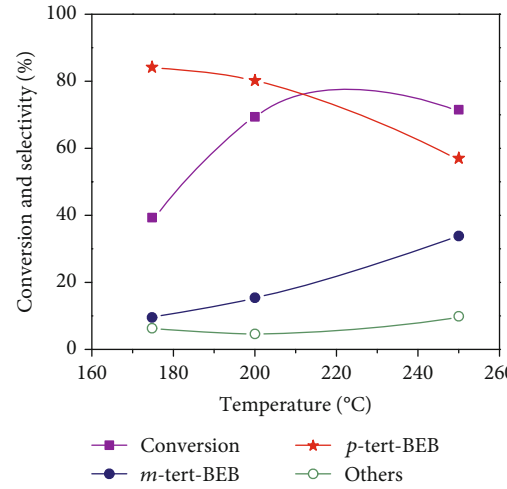

Figure 8: Effect of temperature on ethylbenzene conversion and selectivity of products. (Reaction conditions: catalyst: Al-SBA-15 (US-1 h); feed ratio: 1 : 2; flow rate: 2 ml/h).

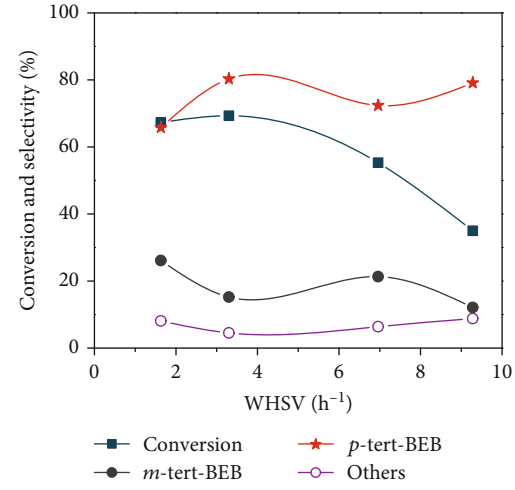

Figure 9: Effect of flow rate on ethylbenzene conversion and selectivity of products (reaction conditions: catalyst: Al-SBA-15 (US-1 h); temperature: 200°C; feed ratio: 1 : 2).

1 : 1 to 1 : 2 is due to enhanced chemisorption of *t*-butanol, thus providing more probability for ethylbenzene to react with *tert*-butyl cation. The decrease in conversion above 1 : 2 is due to the dilution of ethylbenzene by free *t*-butanol in the vapour phase [41]. The selectivity of *m-tert*-BEB

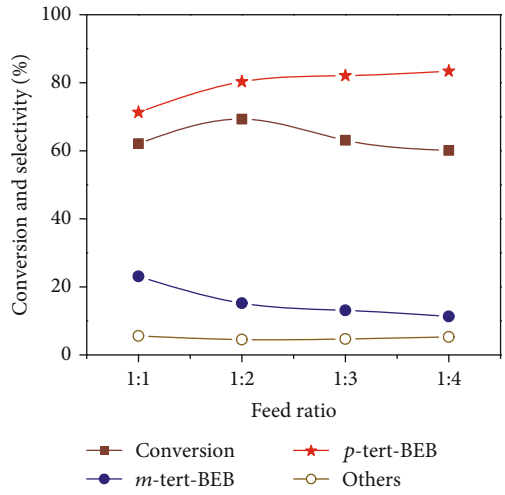

Figure 10: Effect of feed ratio on ethylbenzene conversion and selectivity of products (reaction conditions: catalyst: Al-SBA-15 (US-1 h); temperature: 200°C; flow rate: 2 ml/h).

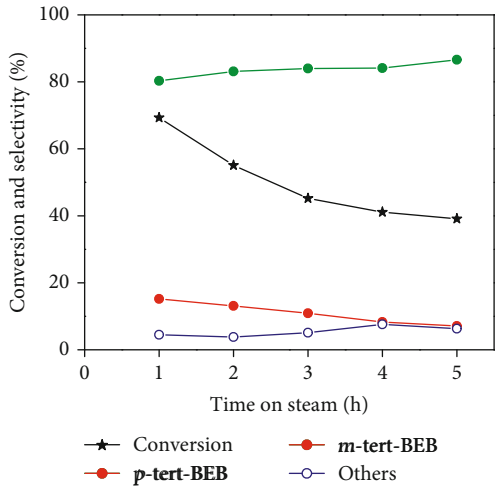

Figure 11: Time-on-stream study on ethylbenzene conversion and selectivity of products on Al-SBA-15 (US-1 h) and feed ratio of 1 : 2.

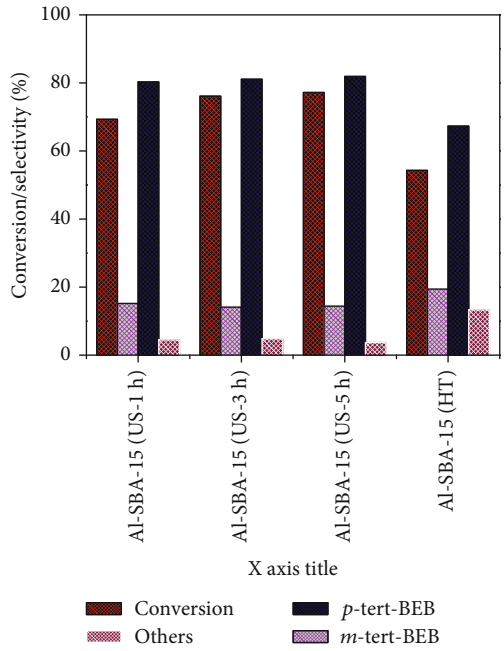

Figure 12: Comparison of Al-SBA-15 US and HT catalysts on ethylbenzene conversion and selectivity of products (reaction conditions: temperature: 200°C; feed ratio: 1 : 2; flow rate: 2 ml/h).

decreases with increasing the content of *tert*-butyl alcohol in the feed. The selectivity of *p-tert*-BEB, therefore, increases with an increase in the content of *tert*-butyl alcohol. This led to a gradual decrease in the adsorption and subsequent isomerization of *p-tert*-BEB [42]. The feed ratio of 1 : 2 was found to be effective for product selectivity.

The effect of time-on-stream on ethylbenzene conversion and the product selectivity was studied at 200°C with a flow rate of 2 ml/h, and the results are displayed in Figure 11. The conversion of ethylbenzene and the selectivity of *m-tert*-BEB decreased with an increase in time-on-stream. This is due to the gradual blocking of active sites by coke. The selectivity of p-tert-BEB increases with an increase in time-on-stream, as its subsequent conversion to m-tert-BEB is gradually suppressed. For the comparison of HT and US (Al-SBA-15) catalysts, they were tested for *tert*-butylation of ethylbenzene in the vapour phase under optimum conditions, and the results are presented in Figure 12. It is observed that the Al-SBA-15 (US) catalysts were determined to be more active than the Al-SBA-15 (HT) catalysts. Since all the ultrasonication method catalysts are equally active, 1 h of sonication is sufficient to yield Al-SBA-15 with high activity.

Noticeably, the *o-tert*-BEB product is not detected due to the steric hindrance offered by the ethyl group. When the ethyl group undergoes resonance interaction with a benzene ring, one ortho position will be sterically blocked, leaving the other steric free. Hence, it may be expected that substitution

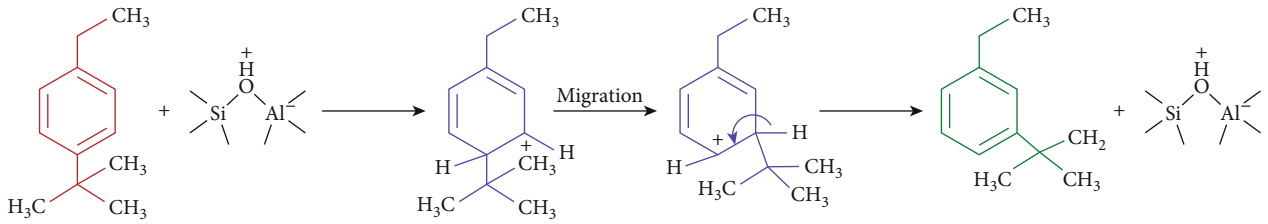

Scheme 2: Possible pathway for the formation of *m-tert*-butylethylbenzene.

may occur at the steric-free ortho carbon. However, the ortho-substituted product is not observed completely. Based on the high steric crowding, either the *tert*-butyl or ethyl groups can be isomerized, but based on the high steric crowding, the *tert*-butyl group might be favoured for isomerization to its ortho position [33]. This isomerization is to proceed not by completely detaching itself from the aromatic ring but by a continuing bond. This isomerization is attributed to the high thermodynamic stability of *m-tert*-BEB compared to *p-tert*-BEB. This type of isomerization is assisted by Brønsted acid sites, as shown in the reaction Scheme 2. Such a mechanism has already been reported by Hemalatha et al. in ZSM-5 catalyst acid sites [43].

4. Conclusions

In conclusion, Al-SBA-15 (US-1, 3, and 5 h) solid acid catalysts were synthesised successfully by the ultrasonication method. All the materials were completely characterised by using XRD, ICP-AES, N_2 sorption analysis, pyridine-FTIR, SEM, TEM, FT-IR, and TGA techniques. The ultrasonication method strongly affects the acidity, structural properties, and morphologies of Al-SBA-15 due to the higher amount of aluminium incorporation. The catalytic activities of these materials were compared with hydrothermally synthesised materials, and it was recognised that the ultrasonication method of synthesised catalysts offered better catalytic performance than HT materials. In the optimal reaction conditions, the US method synthesised materials catalyse the ethylbenzene, with 70% conversion and 82% (*p-tert*-BEB) product selectivity more than that of HT synthesised materials, with 54% conversion and 67% (*p-tert*-BEB) product selectivity. Overall, the ultrasonication method of synthesis offers many advantages over the HT method. This Al-SBA-15 (US) can also be employed as a suitable mesoporous solid acid catalyst for the vapour phase alkylation of alkyl aromatics.

Data Availability

Underlying data supporting the results of our study can be obtained upon request by the corresponding author.

Disclosure

The funders had no role in the design of the study; in the collection, analyses, or interpretation of data; in the writing of the manuscript, or in the decision to publish the results.

Conflicts of Interest

The authors declare no conflict of interest.

Authors' Contributions

Conceptualization and methodology were done by Prabhu A.; data curation was done by Sudha V.; formal analysis was done by Sundaravel B; investigation and editing were done by Pachamuthu M P; supervision was done by Stefano Bellucci.

Acknowledgments

A fruitful discussion with Prof. M. Palanichamy and Prof. V. Murugesan, Anna University, Chennai, India is gratefully acknowledged.

References

[1] A. Corma, "From microporous to mesoporous molecular sieve materials and their use in catalysis," *Chemical Reviews*, vol. 97, no. 6, pp. 2373–2420, 1997.

[2] Y. Liu and T. J. Pinnavaia, "Aluminosilicate mesostructures with improved acidity and hydrothermal stability," *Journal of Materials Chemistry*, vol. 12, no. 11, pp. 3179–3190, 2002.

[3] R. Anwander, "SOMC@PMS. Surface organometallic chemistry at periodic mesoporous silica," *Chemistry of Materials*, vol. 13, no. 12, pp. 4419–4438, 2001.

[4] J. Y. Ying, C. P. Mehnert, and M. S. Wong, "Synthesis and applications of supramolecular-templated mesoporous materials," *Angewandte Chemie, International Edition*, vol. 38, no. 1-2, pp. 56–77, 1999.

[5] A. P. Wight and M. E. Davis, "Design and preparation of organic–inorganic hybrid catalysts," *Chemical Reviews*, vol. 102, no. 10, pp. 3589–3614, 2002.

[6] H. Zhao and H. Han, "Synthesis and characterization of functionalized SBA-15 silica through template removal," *Journal of Solid State Chemistry*, vol. 282, 2020.

[7] R. Bulanek, M. Kubu, J. Vaculik, and J. Cejka, "H/D reactivity and acidity of Brønsted acid sites of MWW zeolites: comparison with MFI zeolite," *Applied Catalysis A: General*, vol. 575, pp. 180–186, 2019.

[8] Y. Zhou, N. Zilkova, M. Shamzhy et al., "Novel approach towards Al-rich AFI for catalytic application," *Applied Catalysis A: General*, vol. 577, pp. 62–68, 2019.

[9] Z. Wu and D. Zhao, "Ordered mesoporous materials as adsorbents," *Chemical Communications*, vol. 47, no. 12, pp. 3332–3338, 2011.

[10] A. Galarneau, D. Desplantier-Giscard, F. DiRenzo, and F. Fajula, "Thermal and mechanical stability of micelle-templated silica supports for catalysis," *Catalysis Today*, vol. 68, no. 1-3, pp. 191–200, 2001.

[11] A. Galarneau, H. Cambon, F. D. Renzo, R. Ryoo, M. Choi, and F. Fajula, "Microporosity and connections between pores in SBA-15 mesostructured silicas as a function of the temperature of synthesis," *New Journal of Chemistry*, vol. 27, no. 1, pp. 73–79, 2003.

[12] D. Zhao, J. Feng, Q. Huo et al., "Triblock copolymer syntheses of mesoporous silica with periodic 50 to 300 angstrom pores," *Science*, vol. 279, no. 5350, pp. 548–552, 1998.

[13] D. Zhao, Q. Huo, J. Feng, B. F. Chmelka, and G. D. Stucky, "Nonionic triblock and star diblock copolymer and oligomeric surfactant syntheses of highly ordered, hydrothermally stable, mesoporous silica structures," *Journal of the American Chemical Society*, vol. 120, no. 24, pp. 6024–6036, 1998.

[14] B. L. Newalker, J. Olanrewaju, and S. Komarneni, "Microwave-hydrothermal synthesis and characterization of zirconium substituted SBA-15 mesoporous silica," *The Journal of Physical Chemistry. B*, vol. 105, no. 35, pp. 8356–8360, 2001.

[15] M. S. Morey, S. O'Brien, S. Schwarz, and G. D. Stucky, "Hydrothermal and postsynthesis surface modification of cubic, MCM-48, and ultralarge pore SBA-15 mesoporous silica with titanium," *Chemistry of Materials*, vol. 12, no. 4, pp. 898–911, 2000.

[16] Z. Luan, J. Y. Bae, and L. Kevan, "Vanadosilicate mesoporous SBA-15 molecular sieves incorporated withN-alkylphenothiazines," *Chemistry of Materials*, vol. 12, no. 10, pp. 3202–3207, 2000.

[17] Z. Luan, E. M. Maes, P. A. Van der Heide, D. Zhao, R. S. Czernuszewicz, and L. Kevan, "Incorporation of titanium into mesoporous silica molecular sieve SBA-15," *Chemistry of Materials*, vol. 11, no. 12, pp. 3680–3686, 1999.

[18] Z. H. Luan, M. Hartmann, D. Y. Zhao, W. Z. Zhou, and L. Kevan, "Alumination and ion exchange of mesoporous SBA-15 molecular sieves," *Chemistry of Materials*, vol. 11, no. 6, pp. 1621–1627, 1999.

[19] Y. Yue, A. Gédéon, J. L. Bonardet, J. B. D'Espinose, J. Fraissard, and N. Melosh, "Direct synthesis of AlSBA mesoporous molecular sieves: characterization and catalytic activities," *Chemical Communications*, vol. 3, pp. 1967-1968, 1999.

[20] J. G. Yu, J. C. Yu, W. K. Ho et al., "Effects of alcohol content and calcination temperature on the textural properties of bimodally mesoporous titania," *Applied Catalysis A: General*, vol. 255, no. 2, pp. 309–320, 2003.

[21] J. C. Yu, J. G. Yu, W. K. Ho, Z. T. Jiang, and L. Z. Zhang, "Effects of F-doping on the photocatalytic activity and microstructures of nanocrystalline TiO2powders," *Chemistry of Materials*, vol. 14, no. 9, pp. 3808–3816, 2002.

[22] J. Yu, M. Zhou, B. Cheng, H. Yu, and X. Zhao, "Ultrasonic preparation of mesoporous titanium dioxide nanocrystalline photocatalysts and evaluation of photocatalytic activity," *Journal of Molecular Catalysis A: Chemical*, vol. 227, no. 1-2, pp. 75–80, 2005.

[23] K. S. Suslick and G. J. Price, "Applications of ultrasound to materials chemistry," *Annual Review of Materials Science*, vol. 29, pp. 295–326, 1999.

[24] E. B. Flint and K. S. Suslick, "The temperature of cavitation," *Science*, vol. 253, no. 5026, pp. 1397–1399, 1991.

[25] M. Run, S. Wu, and G. Wu, "Ultrasonic synthesis of mesoporous molecular sieve," *Microporous and Mesoporous Materials*, vol. 74, no. 1-3, pp. 37–47, 2004.

[26] S. K. Lee, J. Lee, J. Joo et al., "Rapid sonochemical synthesis of spherical-shaped mesoporous SBA-15 silica and Ti-incorporated SBA-15 silica materials," *Journal of Industrial and Engineering Chemistry*, vol. 9, pp. 83–88, 2003.

[27] Y. Q. Wang, L. X. Yin, O. Palchik, Y. R. Hacohen, Y. Koltypin, and A. Gedanken, "Rapid synthesis of mesoporous yttrium –zirconium oxides with ultrasound irradiation," *Langmuir*, vol. 17, no. 13, pp. 4131–4133, 2001.

[28] M. Sathish and R. P. Viswanath, "Ultrasonic-mediated preparation of mesoporous crystalline CdS nanoparticle," *Chemistry Letters*, vol. 36, no. 7, pp. 948-949, 2007.

[29] Z. Wang, H. Ling, J. Shi et al., "Acidity enhanced [Al]MCM-41 via ultrasonic irradiation for the Beckmann rearrangement of cyclohexanone oxime to ε-caprolactam," *Journal of Catalysis*, vol. 358, pp. 71–79, 2018.

[30] I. Rakngam, N. Osakoo, J. Wittayakun et al., "Properties of mesoporous Al-SBA-15 from one-pot hydrothermal synthesis with different aluminium precursors and catalytic performances in xylose conversion to furfural," *Microporous and Mesoporous Materials*, vol. 317, 2021.

[31] A. Prabhu, B. Sundaravel, and M. P. Pachamuthu, "Acylation of isobutylbenzene with acetic anhydride on AlKIT-6 mesoporous acid catalyst," *Materials Science for Energy Technologies*, vol. 4, pp. 128–135, 2021.

[32] M. Pasupathi, N. Santhi, M. P. Pachamuthu, G. Alamelu Mangai, and C. Ragupathi, "Aluminium and titanium modified mesoporous TUD-1: a bimetal acid catalyst for Biginelli reaction," *Journal of Molecular Structure*, vol. 1160, pp. 161–166, 2018.

[33] V. Umamaheswari, M. Palanichamy, and V. Murugesan, "Isopropylation of m-cresol over mesoporous Al–MCM-41 molecular sieves," *Journal of Catalysis*, vol. 210, no. 2, pp. 367–374, 2002.

[34] J. G. Drobny, *Handbook of Thermoplastic Elastomers*, Elsevier, New York, NY, USA, 1st Ed. edition, 2007.

[35] J. Ma, L.-S. Qiang, J.-F. Wang, X.-B. Tang, and D.-Y. Tang, "Effect of different synthesis methods on the structural and catalytic performance of SBA-15 modified by aluminum," *Journal of Porous Materials*, vol. 18, no. 5, pp. 607–614, 2011.

[36] G. Chandrasekar, M. Hartmann, M. Palanichamy, and V. Murugesan, "Extrusion of AlSBA-15 molecular sieves: an industrial point of view," *Catalysis Communications*, vol. 8, no. 3, pp. 457–461, 2007.

[37] A. Vinu, B. M. Devassy, S. B. Halligudi, W. Böhlmann, and M. Hartmann, "Highly active and selective AlSBA-15 catalysts for the vapor phase tert-butylation of phenol," *Applied Catalysis A: General*, vol. 281, no. 1-2, pp. 207–213, 2005.

[38] F. Akti, "Effect of kaolin on aluminum loading success in synthesis of Al-SBA-15 catalysts: activity test in ethanol dehydration reaction," *Microporous and Mesoporous Materials*, vol. 294, 2020.

[39] C. H. Qiang and Z. D. Yuan, "One-step direct synthesis of mesoporous aluminosilicates Al-SBA-15 with cage-like macropores by using micrometer-sized aluminum balls," *Science in China Series B Chemistry*, vol. 52, pp. 1090–1096, 2009.

[40] S. A. A. Vandarkuzhali, B. Viswanathan, M. P. Pachamuthu, and S. C. Kishore, "Fine Copper Nanoparticles on Amine Functionalized SBA-15 as an Effective Catalyst for Mannich Reaction and Dye Reduction," *Journal of Inorganic and Organometallic Polymers and Materials*, vol. 30, pp. 359–368, 2020.

[41] V. M. Palanichamy, B. Arabindoo, and V. Murugesan, "Vapour phase alkylation of ethylbenzene witht-butyl alcohol over mesoporous Al-MCM-41 molecular sieves," *Journal of Chemical Sciences*, vol. 114, pp. 203–212, 2002.

[42] A. Sakthivel, S. K. Badamali, and P. Selvam, "para-Selective t-butylation of phenol over mesoporous H-AlMCM-41," *Microporous and Mesoporous Materials*, vol. 39, no. 3, pp. 457–463, 2000.

[43] P. Hemalatha, M. Ganesh, M. Palanichamy et al., "Effects of crystallinity of ZSM 5 zeolite onpara selective tert butylation of ethylbenzene," *Chinese Journal of Catalysis*, vol. 34, pp. 294–304, 2013.